

Fig. 3. Experimental procedures for quantitative real-time PCR analysis.

the quantitative real-time PCR. Total RNA samples were extracted from heads 100 in total everytime of the fruit fly every two hours during the first day in L:D=12:12 (a light/dark cycle of 12 h and 12 h) and the second day in DD (constant darkness) (Fig. 3).

We eventually found four alternative splicing sites for *Drosophila period* mRNA. Three successive introns at the C-terminal region were denoted as the site #1, #2, and #3, which involve 70-base, 64-base, and 58-base, respectively. The alternative splicing site #4 has been previously reported as a 89-base site in the 3' UTR. We succeeded to identify all of 16 possible splicing variants produced by all the insertion/deletion combinations at the 4 respective sites. Based on these gene structures, we predicted that there are 5 PERIOD protein isoforms. For real-time PCR, the alternative splicing sites were examined to quantify the insertion-type and deletion-type mRNAs.

We designed PCR primers for quantification of the each insertion- and deletion-type mRNA isoforms. For *Drosophila period* mRNA genes, real-time PCR analyses revealed that the total mRNA exhibits the expression peaks at ZT 13 or CT 13. ZT (zeitgeber time) denotes the time entrained by environmental time cues, whereby lights on is ZT0 and lights off is ZT17. CT (circadian time) denotes the time entrained by no environmental time cues. As to the quantification of each deletion-type isoform at the alternative splicing sites #1, #2, and #3, the expression profiles were found to be similar to that of the total mRNA described above. On the other hand, in the quantifications of insertion-type isoforms, a unique sub-peak was found at the morning. The evening peak appeared to have rather larger sub-peaks. However, it should be noted that these sub-peaks rapidly disappeared to place the condition from LD to DD. The analysis of biosynthesis of mRNA genes clearly indicated that the alternative splicing events at the sites #1, #2, and #3 are light-sensitive. This should be followed by PERIOD protein biosynthesis.

To elucidate whether or not the morning peak is made by PERIOD protein isoforms, we carried out the western blotting analyses. We focused on the insertion and deletion of the alternative splicing site #1. The deletion-type PERIOD protein was denoted as type-A, while the insertion-type was type-C (Fig. 2B). They have different amino acid sequences at the C-terminals. The antibodies used were anti PERIOD N-terminus antibody and newly prepared anti PERIOD type-C mouse monoclonal antibody.

We carried out the western blotting analysis for quantification profile of the type-C PERIOD protein isoforms. We depicted an expression profile for each type of

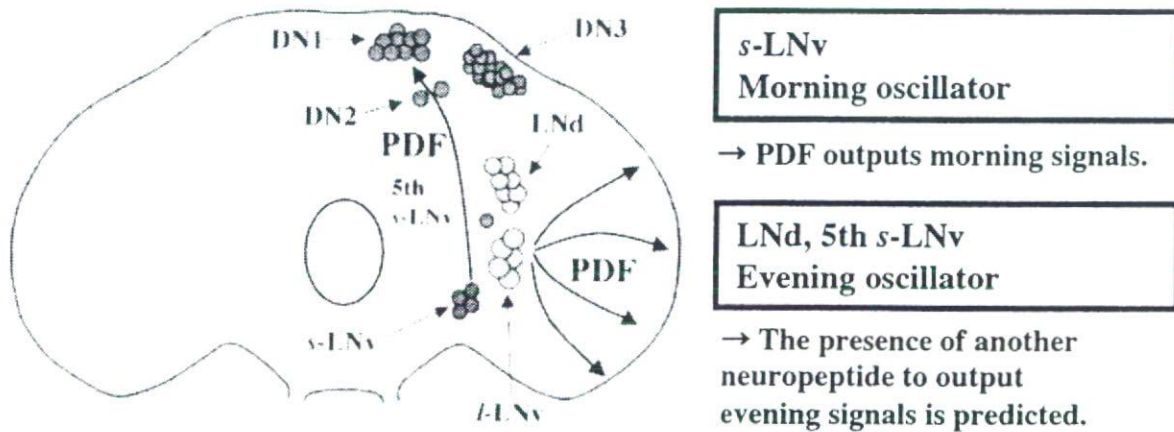


Fig. 4. Schematic figures of *D. melanogaster* PERIOD

isoforms. The peak profiles were found to differ under the conditions of either LD or DD. Under the L:D=12:12 condition, there were two protein peaks at ZT 5 and ZT 15. The profile was definitely different from that of PERIOD type-A. Under DD condition the bimodal expression was disappeared. At the first day in DD, the expression profile of PERIOD type-C came to be similar to that of type-A. Interestingly, the results suggested that biosyntheses of type-C mRNA and proteins are light-sensitive, but not thermo-sensitive.

For the *period* mRNA genes in the silk moth *Bombyx mori*, we have also identified three alternative splicing sites containing 15-base, 15-base, and 129-base. The isoform produced by the alternative splicing at the site #3 were found to differ in their production. The expression of insertion-type peaks in the morning, whereas that of deletion-type peaks in the evening. Therefore these *period* isoforms are expected to involved in the morning and evening oscillators.

All the present results suggest that the specific set of PERIOD isoforms should be required for either morning oscillator or evening oscillator. Since PDF knockout flies exhibit only evening activity in the locomotor rhythm, PDF-expressing neurons should drive the morning oscillator. Although we have not revealed which neuronal group expresses PERIOD type-C, it is predicted that PERIOD type-C expresses in either *s*-LNv or LNd and 5th *s*-LNv (Fig. 4). The evening oscillator is said to be present at the LNd and 5th *s*-LNv, and these neurons do not express PDF. The model strongly suggests the presence of another unidentified neuropeptide to output evening activity (Fig. 4).

## References

1. Honda, T., Matsushima, A., Sumida, K., Chuman, Y., Sakaguchi, K., Onoue, H., Meinertzhagen, I.A., Shimohigashi, Y., Shimohigashi, M. (2006) *J. Comp. Neurol.*, **499**, 404-421.
2. Matsushima, A., Takano, K., Yoshida, T., Takeda, Y., Yokotani, S., Shimohigashi, Y., and Shimohigashi, M. (2007) *J. Biochem.*, **141**, 867-877.
3. Matsushima, A., Sato, S., Chuman, Y., Takeda, Y., Yokotani, S., Nose, T., Shimohigashi, M., and Shimohigashi, Y. (2004) *J. Pept. Sci.*, **10**, 82-91.
4. Takeda, Y., Chuman, Y., Shirasu, N., Sato, S., Matsushima, A., Kaneki, A., Tominaga, Y., Shimohigashi, Y., and Shimohigashi, M. (2004) *Zool. Sci.*, **21**, 903-915.
5. Grima, B., Chelot, E., Xia, R., and Rouyer, F. (2004) *Nature*, **43**, 869-873.
6. Stoleru, D., Peng, Y., Agosto, J., and Rosbash, M. (2004) *Nature*, **43**, 862-868.

## Differential Receptor Recognition by Dmt-Containing Enkephalin Dimers Cross-Linked by Phenylenediamines

Nobuko Inokuchi<sup>1</sup>, Kaname Isozaki<sup>1</sup>, Yuko Tsuda<sup>2</sup>, Yoshio Okada<sup>2</sup>, Satoshi Osada<sup>3</sup>, Takeru Nose<sup>1</sup>, Tommaso Costa<sup>4</sup> and Yasuyuki Shimohigashi<sup>1</sup>

<sup>1</sup>Laboratory of Structure-Function Biochemistry, Kyushu University, Fukuoka 812-8581, Japan, <sup>2</sup>Faculty of Pharmaceutical Sciences and High Technology Research Center, Kobe Gakuin University, Nishi-ku, Kobe 651-2180, Japan, <sup>3</sup>Department of Chemistry and Applied Chemistry, Saga University, Saga 840-8502, Japan, and <sup>4</sup>Laboratorio di Farmacologia, Istituto Superiore di Sanità, Viale Regina Elena 299, Roma, Italy  
e-mail: shimoscc@mbx.nc.kyushu-u.ac.jp

*Opioid receptors such as  $\delta$ ,  $\mu$ , and  $\kappa$  subtypes are suggested to exist as a dimer, but its molecular determinants are still unknown. We previously reported that bivalent ligands with two binding cores cross-linked by a spacer exhibited the bivalent interaction mode for each specific receptor. In particular, the inactive enkephalin fragment Tyr-D-Ala-Gly was found to activate the  $\mu$  receptor by its dimerization. In the present study, we attempted to prepare the structurally constrained analogs of DTRE2 in order to attain a molecular tool for evaluating the organization of receptor dimerization.*

**Keywords:** enkephalin, enkephalin dimers, G protein-coupled receptors (GPCRs), opioid receptors

### Introduction

G protein-coupled receptors (GPCRs) comprise the largest family of transmembrane receptors. Opioid receptors (ORs) such as  $\delta$ ,  $\mu$ , and  $\kappa$  are member of GPCR and all of these receptor subtypes are suggested to exist as dimers. Many lines of evidence have revealed that opioid receptors are present as either homodimer or heterodimer in rat brain. A bivalent ligand with two binding cores cross-linked by a spacer would be capable to interact with two receptor molecules simultaneously [1]. This would lead the increase in affinity, selectivity, and probably biological activity.

We previously reported that DTRE2, (H-Tyr-D-Ala-Gly-NH-CH<sub>2</sub>-)<sub>2</sub>, a dimer of inactive N-terminal tripeptide of enkephalin (TRE) cross-linked by ethylenediamine, bound to the  $\mu$  receptor considerably strongly [2]. In this DTRE2 dimer, the structural element essential for receptor binding is definitely the N-terminal Tyr

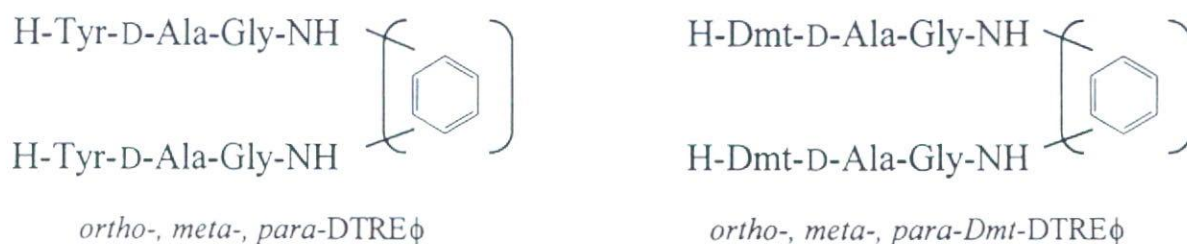


Fig. 1. Chemical structure of DTRE $\phi$  and Dmt-DTRE $\phi$

residues.

### Results and Discussion

We first dimerized TRE monomer with *ortho*-, *meta*-, and *para*-phenylenediamines, and then replaced Tyr with 2',6'-dimethyl-L-Tyr (Dmt) [3]. These Dmt-DTRE $\phi$  analogs were synthesized by three-step coupling reaction; *i.e.*, coupling, elongation, and then deblocking. Here, ' $\phi$ ' designates the benzene ring. Dmt-DTRE $\phi$  dimers synthesized were purified by silica gel column chromatography (Silica Gel 60, 1.6 x 60 cm) eluted with CHCl<sub>3</sub>:MeOH (19:1 v/v), and protected peptides were verified by the elementary analysis. The final products of Dmt-DTRE $\phi$  dimers were purified by preparative RP-HPLC with a preparative column (25 x 250 mm, Cica-Merck LiChrospher RP-18(e), 5  $\mu$ m). The purity of peptides was verified by analytical (RP)-HPLC (4 x 250 mm, Cica-Merck LiChrospher 100RP-18, 5  $\mu$ m). The mass spectra were measured on a mass spectrometry Voyager<sup>TM</sup> DE-PRO (PerSeptive Biosystems Inc., Framingham, MA) with the method of matrix-assisted laser desorption ionization time-of-flight (MALDI-TOF) to identify the mass speak of final compounds.

The opioid receptors are known to couple with G $_{\alpha o}$  protein, which is heterogeneous  $\alpha\beta\gamma$  trimer with a GDP molecule bound to the  $\alpha$ -subunit noncovalently. In the present study, we utilized not only rat  $\delta$ ,  $\mu$  and  $\kappa$  ORs, but also G $_{\alpha o}$ -fused ORs in order to assess the receptor activation more effectively.

All receptors were transiently expressed on COS-7 cells, and the membrane preparations were used for saturation binding assay, competitive binding assay, and [<sup>35</sup>S]GTP $\gamma$ S functional assay. The expression efficiency of  $\delta$ ,  $\mu$ ,  $\kappa$ -OR and  $\delta$ ,  $\mu$ ,  $\kappa$ -OR-G $_{\alpha o}$  were evaluated by the saturation binding assay using [<sup>3</sup>H]deltorphine II for  $\delta$  receptor, [<sup>3</sup>H]DAGO for  $\mu$  receptor, and [<sup>3</sup>H]U69593 for  $\kappa$  receptor. The dissociation constant  $K_d$  of each receptor was calculated from the Scatchard analysis. It was found that both fused and non-fused receptors interact with the ligands equally well.

In the receptor binding assay, newly synthesized *ortho*- and *meta*-Dmt-DTRE $\phi$  dimers exhibited drastically increased binding affinity for  $\mu$  receptor subtype (Table 1). In particular, *ortho*-Dmt-DTRE $\phi$  became extremely active (almost 80 times more potent than *ortho*-DTRE $\phi$ ) for the  $\mu$  opioid receptor. This is quite likely, since the parent *ortho*-DTRE $\phi$  was considerably potent for the  $\mu$  receptor (Table 1), despite that other DTRE dimers (*meta*-DTRE $\phi$  and *para*-Dmt-DTRE $\phi$ ) were almost completely inactive. Indeed, *para*-Dmt-DTRE $\phi$  exhibited no affinity for all the receptor subtypes in spite of Dmt-substitution.

However, surprisingly, *meta*-Dmt-DTRE $\phi$  increased remarkably the binding affinity for the  $\mu$  receptors. Its IC<sub>50</sub> value was almost compatible with that of *ortho*-Dmt-DTRE $\phi$ . The reason of this very high binding activity attained by *meta*-Dmt-DTRE $\phi$  is quite unexpected, since its Tyr-containing analogue

Table 1. Binding potency of Dmt DTRE dimers with ORs.

	Binding Potency (IC <sub>50</sub> : nM)					
	μ: [ <sup>3</sup> H]DAMGO		δ: [ <sup>3</sup> H]Deltorphin II		κ: [ <sup>3</sup> H]U-69593	
<i>ortho</i> -Dmt-DTREφ	1.05 ± 0.98	18.6 ± 8.36	6.05 ± 3.06			
<i>ortho</i> -DTREφ	78.4 ± 0.60	1430 ± 55	>10,000			
<i>meta</i> -Dmt-DTREφ	1.59 ± 0.89	37.6 ± 36.4	6.06 ± 1.19			
<i>meta</i> -DTREφ	>10,000	>10,000	N. B. *			
<i>para</i> -Dmt-DTREφ	>10,000	N. B. *	N. B. *			
<i>para</i> -DTREφ	N. B. *	N. B. *	N. B. *			
Deltorphin II	2.26 ± 0.98	-	-			
DAMGO	-	5.36 ± 1.88	-			
U-69593	-	-	5.80 ± 3.05			

\*N.B.: Not Bound

*meta*-DTREφ was inactive. The activation by the Tyr→Dmt substitution is so dramatic, since the structural change is very subtle in their chemical structures. Apparently, the incorporation of Dmt brought about the conformation change, in which Dmt constrained the steric structure of dimer only to the bioactive conformation.

Dmt-DTREφ dimers were also examined in the [<sup>35</sup>S]GTPγS binding assay to assess their receptor activation ability. For the Gα<sub>o</sub>-fused μ receptors, *para*-Dmt-DTREφ was almost completely inactive as expected from the receptor binding activity. On the other hand, *ortho*-Dmt-DTREφ and *meta*-Dmt-DTREφ were both very active in this functional assay. *ortho*-Dmt-DTREφ exhibited very high activity (approximately 140% *E*<sub>max</sub> of μ-ligand DAGO) for the μ receptor. When we

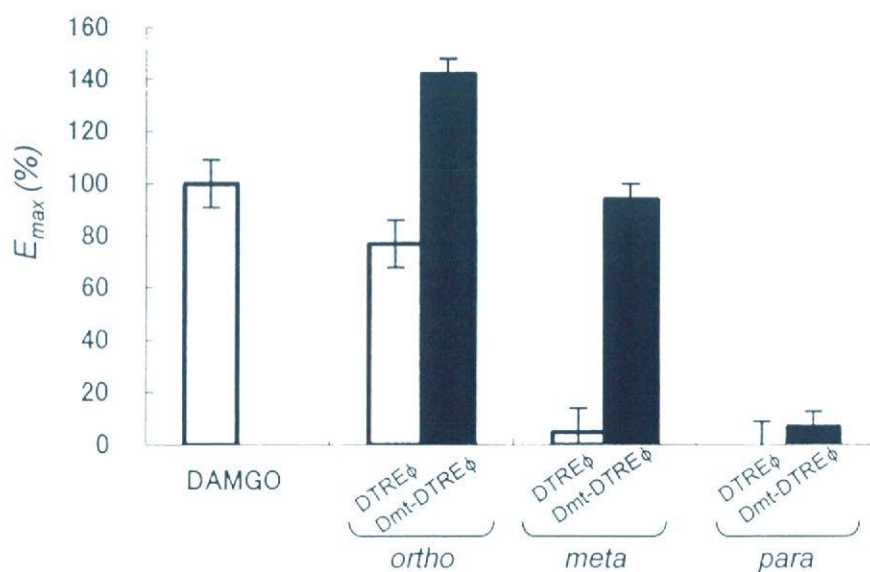


Fig. 2. Stimulation of [<sup>35</sup>S]GTPγS binding to μ-OR-Gα<sub>o</sub> by Dmt-DTRE dimers.

compared its activity with that of DTRE $\phi$  dimer, about 60% activity enhancement was attained by the Tyr $\rightarrow$ Dmt substitution. It is now important to examine the question whether or not this activity enhancement was brought about by the bivalent interaction.

*meta*-Dmt-DTRE $\phi$  was found to be biologically active, implying that this analogue is a distinct agonist. Although Tyr  $\rightarrow$  Dmt substitution for *meta*-DTRE $\phi$  cause this dramatic activity conversion, namely, from the inactivity to the high activity almost equivalent to DAGO, the exact reason is not clear. At this moment, it is important to clarify whether or not *ortho*-Dmt-DTRE $\phi$  and *meta*-Dmt-DTRE $\phi$  do interact with the  $\mu$ -receptor in the same way. To answer these question, detailed structure-activities studies of these dimeric peptides are in progress in our laboratory.

### Reference

1. Shimohigashi, Y., Costa, T., Chen, H.-C., and Rodbard, D. (1982) *Nature*, **297**, 333-335.
2. Shimohigashi, Y., Ogasawara, T., Koshizaka, T., Waki, M., Kato, T., Izumiya, N., Kurono, M., and Yagi, K. (1987) *Biochem. Biophys. Res. Commun.*, **146**, 1109-1115.
3. Okada, Y., Tsuda, Y., Fujita, Y., Yokoi, T., Sakaki, Y., Ambo, A., Konishi, R., Nagata, M., Salvadori, S., Jinsmaa, Y., Bryant, S.D. (2003) *J. Med Chem.* **46**, 3201-3209

## Structural Requirement of Housefly FMRFamide Peptides in Its Receptor Activation

Ayami Matsushima<sup>1</sup>, Yukie Koretsune<sup>1</sup>, Atsushi Kaneki<sup>1</sup>, Kaname Isozaki<sup>1</sup>,  
Miki Shimohigashi<sup>2</sup>, and Yasuyuki Shimohigashi<sup>1</sup>

<sup>1</sup>Faculty and Graduate School of Sciences, Kyushu University, Fukuoka 812-8581,  
Japan, <sup>2</sup>Division of Biology, Faculty of Science, Fukuoka  
University, Fukuoka 814-0180, Japan  
e-mail: ayamiscc@mbox.nc.kyushu-u.ac.jp

*FMRFamide peptides contain the C-terminal structure of Phe-Met-Arg-Phe-NH<sub>2</sub>. We have recently achieved the cDNA cloning of FMRFamide and its receptor in the housefly *Musca domestica*. In the present study, we performed the structure-activity studies by using the truncated analogues of *Musca* FMRFamides and site-directly mutated *Musca* FMRMamide receptor. It was shown that the C-terminal hexapeptide sequence of DNFMRF-NH<sub>2</sub> is crucial for receptor activation.*

**Keywords:** FMRFamide, G protein-coupled receptor, insect, reporter gene assay

### Introduction

Peptides containing C-terminal FMRF-NH<sub>2</sub> and its related structures are members of a large family of structurally related peptides found in both invertebrate and vertebrate species. In insects, these peptides are called FMRFamide-related peptides (FaRPs) and three major families have been reported to date, including FMRFamides, sulfakinins, and myosuppressins [1]. We have recently elucidated the whole structure of FaRPs in the housefly *Musca domestica* by the cDNA cloning analysis, and found 13 kinds of 17 FaRPs [2]. It is remarkable that only one peptide is common to both *Drosophila* FMRFamides and *Musca* FMRFamides, although both species belong to the same taxonomic groups of Diptera.

We succeeded recently in cDNA cloning of the *Musca* FMRFamide receptor (designated as *Musca* FR) by reverse transcribe-PCR using degenerated primers designed from the *Drosophila* FR cDNA sequence [3]. This is the second fastest finding of insect FRs. *Musca* FR is a member of G protein-coupled receptor (GPCR), and is very similar to *Drosophila* FR. The amino acid sequence identity and similarity of these two FRs are 64% and 83%, respectively. These FRs are predicted as a class-A GPCR by the computer-assisted Internet program GRIFFIN (<http://griffin.cbrc.jp/>). It should be noted that no disulfide bond is present between the first extracellular loop (EL1) and EL2, unlike most of other GPCRs.

We have established a novel reporter gene assay system for FRs and FMRFamide peptides by using a cAMP response element (CRE)-luciferase construct. *Musca* FR was found to be activated by all of 13 kinds of *Musca* FMRFamides, but the

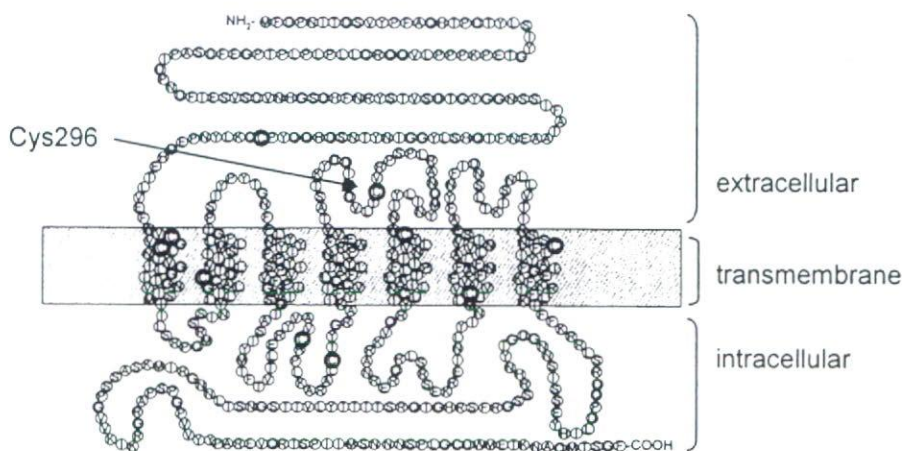


Fig. 1. The structural topology prediction of the *Musca* FMRFamide receptor.

levels of luciferase activities of FaRPs found to vary and PDNFMRF-NH<sub>2</sub> showed the highest activity. In the present study, we performed the structure-activity studies to elucidate the structural elements important for receptor activation. To this end, we prepared the truncated analogues of PDNFMRF-NH<sub>2</sub>. The site-directly mutated *Musca* FR with Cys→Ala substitution in EL2 was also prepared to examine whether or not the mutant FR attains a full activation.

### Results and Discussion

As to PDNFMRF-NH<sub>2</sub>, one of *Musca* FMRFamide peptides, we synthesized the truncated analogues DNFMRF-NH<sub>2</sub> and NFMRF-NH<sub>2</sub>. For direct measurement of the specific activity by the reporter gene assay, HEK293 cells expressing *Musca* FR was used together with a CRE-luciferase construct. N-terminal Pro(=P)-lacking DNFMRF-NH<sub>2</sub> was found to elicit almost the same activity as the parent PDNFMRF-NH<sub>2</sub>. However, NFMRF-NH<sub>2</sub> lacking N-terminal Pro-Asp(=PD) dipeptide showed significantly weakened activity (about 5-fold less active). These results clearly indicated that the minimum bioactive structure of PDNFMRF-NH<sub>2</sub> is DNFMRF-NH<sub>2</sub>, but not NFMRF-NH<sub>2</sub>, and thus the Asp residue adjacent to Pro and Asn is definitely important for this activation. It should be noted that PDNFMRF-NH<sub>2</sub> is the sole peptide that is encoded in both *Musca* and *Drosophila* FMRFamides genes. PDNFMRF-NH<sub>2</sub> may be the most sophisticated peptide to activate fly FR *in vivo*, and the other fly species may have a FMRFamide peptide of this amino acid sequence.

The disulfide bond between EL1 and EL2 has been said to be important to retain a bioactive activation conformation of GPCR. However, in *Musca* FR, there appears no such a disulfide SS bond. This is because Cys296 in EL2 is a sole Cys residue, and there is no Cys in EL1 (Fig. 1). In the present study, we prepared the Cys296→Ala mutant FR. As a result, the mutant receptor was found to retain the full activity. The present results implied some other interactions between EL1 and EL2 may compensate for the disulfide bonding to keep up the receptor activation conformation.

### References

1. Nässel, D. R. (2002) *Prog. Neurobiol.*, **68**, 1-84.
2. Matsushima, A., Takano, K., Yoshida, T., Takeda, Y., Yokotani, S., Shimohigashi, Y., and Shimohigashi, M. (2007) *J. Biochem.*, **141**, 867-877.
3. Matsushima, A., Koretsune, Y., Kaneki, A., Isozaki, K., Shimohigashi, M., and Shimohigashi, Y. (2006) *Peptide Science 2006*, 174.

## Optimization of the N-Terminal Group of Ac-RYYRIK-NH<sub>2</sub> as ORL1 Receptor Antagonist

Jinglan Li<sup>1</sup>, Kaname Isozaki<sup>1</sup>, Ayami Matsushima<sup>1</sup>, Takeru Nose<sup>1</sup>,  
Tommaso Costa<sup>2</sup>, and Yasuyuki Shimohigashi<sup>1</sup>

<sup>1</sup>Laboratory of Structure-Function Biochemistry, Kyushu University, Fukuoka  
812-8581, Japan, <sup>2</sup>Laboratorio di Farmacologia, Istituto Superiore  
di Sanità, Viale Regina Elena 299, Roma, Italy  
email: Lijinglanscc@mbox.nc.kyushu-u.ac.jp

*Ac-RYYRIK-NH<sub>2</sub> is firstly reported as an antagonist that inhibits the nociceptin activities mediated through ORL1 receptor. However, Ac-RYYRIK-NH<sub>2</sub> has also acts as a partial agonist. We previously reported that the N-terminal moiety of this peptide is crucially important for specific receptor interaction, and found that isovareloyl-RYYRIK-NH<sub>2</sub> exhibits high affinity and strong antagonist activity. In the present study, we intended to determine the structural elements required for this antagonist by optimizing the acyl group for antagonist activity.*

**Keywords:** antagonist, nociceptin, ORL1 (opioid receptor like 1), partial agonist

### Introduction

Nociceptin, a 17-mer neuropeptide with the sequence FGGFTGARKSARKL ANQ, is an endogenous ligand of the ORL1 (opioid receptor-like 1) receptor. This receptor belongs to the G protein-coupled receptor (GPCR) superfamily, and couples specifically with G<sub>i</sub> or G<sub>o</sub> protein. Nociceptin induces hyperalgesia, and the nociceptin/ORL1 ligand-receptor system is also involved in many other physiological functions such as analgesia in the spinal cord and anti-opioid effects in the brain [1]. In general, for better understanding of such different functions of biologically active peptides, it is imperative to obtain a highly selective and specific receptor antagonist. Antagonist is an important and indispensable molecular tool for investigation of the inhibition mechanism of receptor activation. Because of the intrinsic hyperalgesic activity of nociceptin, its antagonists are expected to be highly effective analgesics.

Acetyl hexapeptide amide Ac-Arg-Tyr-Tyr-Arg-Ile-Lys-NH<sub>2</sub> (Ac-RYYRIK-NH<sub>2</sub>) has been reported as an effective nociceptin antagonist [2]. Since Ac-RYYRIK-NH<sub>2</sub> displaces [<sup>3</sup>H]nociceptin in a dose-dependent manner, these two peptides Ac-RYYRIK-NH<sub>2</sub> and nociceptin should share and thus compete for the binding site in ORL1 receptor. However, Ac-RYYRIK-NH<sub>2</sub> *per se* was found to exhibit partial agonist activity in the [<sup>35</sup>S]GTPγS binding assay [3].

In our previous study, based on the fact that the analogue lacking the acetyl group, H-RYYRIK-NH<sub>2</sub>, showed drastically reduced binding potency, we noted the importance of the N-terminal acetyl group, CH<sub>3</sub>CO-, as a structural element essential for binding to ORL1 receptor. Then, we found that isovareloyl-RYYRIK-NH<sub>2</sub> with

substituted N-terminal isovareloyl group,  $(\text{CH}_3)_2\text{CH}_2\text{CO}-$ , exhibited strong antagonist activity as compared to  $\text{Ac-RYYRIK-NH}_2$ .

In the present study, focusing on the N-terminal isovareloyl group of the strongest antagonist, we attempted to design-synthesize even stronger antagonists. We selected seven different acyl groups with slightly changed structure (Fig. 1) to evaluate the influences to their binding potency and activation efficacy. We here describe the structure-activity relationships of acyl-RYYRIK-NH<sub>2</sub> peptides for the best selection of ORL1 nociceptin antagonism.

## Results and Discussion

All acyl-RYYRIK-NH<sub>2</sub> analogues were prepared by the SPS method using Fmoc-amino acids. N-Terminal acylation was carried out at the end of each synthesis cycle by using the corresponding carboxylic acid (R-COOH). Peptides were liberated from the resin and protecting groups by Reagent K, and purified by gel filtration followed by reversed-phase HPLC. The measurement of MALDI-TOF mass spectroscopy guaranteed the theoretical value of the molecular weight of each peptide synthesized (Table 1).

For the receptor binding assay and [<sup>35</sup>S]GTPγS binding assay, we used the membrane preparations from the COS-7 cells expressing human ORL1 fused with the α subunit of G<sub>o</sub> protein (G<sub>αo</sub>). This fusion receptor ORL1-G<sub>αo</sub> was constructed to evaluate the peptides effectively in the [<sup>35</sup>S]GTPγS binding assay. We could verify the receptor population sufficiently enough to carry out a series of binding assays; *i.e.*, the saturation binding assay, the competitive binding assay, and the GTPγS binding assay.

Referring the chemical structure of the isovareloyl group, we designed three different types of N-terminal acyl groups for RYYRIK-NH<sub>2</sub>. Firstly, to evaluate the methyl group at the γ position as a trigger for receptor binding and activation, C<sub>β</sub> was converted to much more electrically negative atoms N, O, and S. Secondly, focusing on the chemical bond between C<sub>α</sub> and C<sub>β</sub>, the angelicyl group with the C=C double bond and the tetrolicyl group with the triple C≡C bond were introduced. Thirdly, we placed the amino acid valine, which contains the carbon backbone structure of the isovareryl group. L-Val and D-Val were used to evaluate the difference induced by their spatial variety.

In the radio-ligand receptor binding assay, methylthio-RYYRIK-NH<sub>2</sub> was found to exhibit the strongest activity with the IC<sub>50</sub> value of 0.74 nM (Table 2).

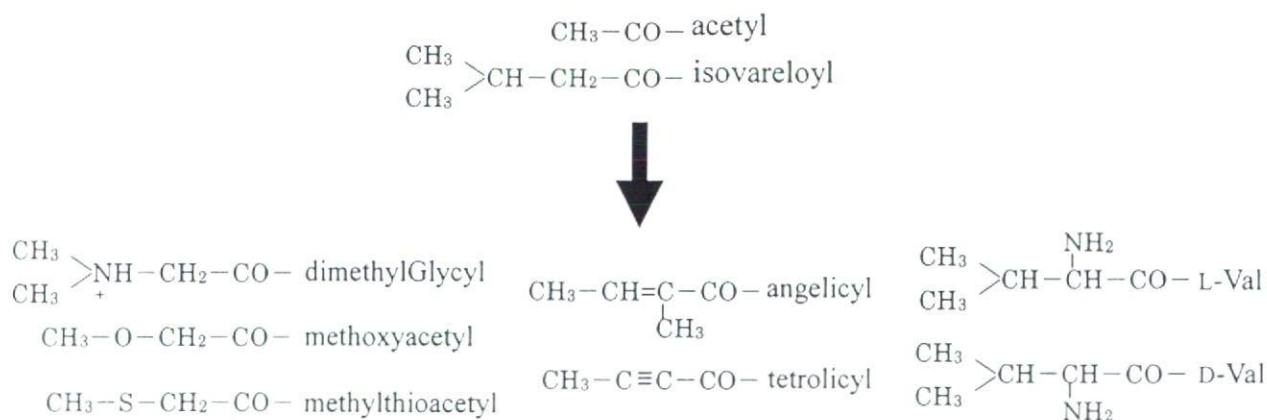


Fig. 1. Chemical structure of N-terminal acyl group for RYYRIK-NH<sub>2</sub>.

Table 1. Molecular weight determination of acyl-RYYRIK-NH<sub>2</sub> peptides by the MALDI-TOF mass spectroscopy.

acyl-RYYRIK-NH <sub>2</sub> (acyl groups)	MALDI-TOF-MS	
	Found (m/z)	Theoretical (m+H <sup>+</sup> )
acetyl	940.39	940.55
isovareloyl	982.03	982.20
dimethylGlycyl	983.07	983.62
methoxyacetyl	969.07	970.94
methylthioacetyl	986.07	986.82
angelicyl	979.07	980.79
tetrolicyl	963.07	964.97
L-Val	996.07	997.96
D-Val	996.07	997.04

This analogue is as strong as the parent peptide Ac-RYYRIK-NH<sub>2</sub> (Table 2). The peptide having the methoxy acetyl group also showed a considerably high binding potency, but the *N,N*-dimethyl glycyl analogue showed almost 100 times reduced binding potency as compared to the isovareloyl analogue. A very high receptor binding affinity observed for methylthioacetyl-RYYRIK-NH<sub>2</sub> made us enthusiastic about its biological activity, anticipating a pure antagonism. However, unfortunately, this expectation was immediately downed, since the analogue was found to activate the ORL1-G<sub>αo</sub> receptor up to approximately 50% in the GTPγS binding assay. The result implied that this analogue is only a partial agonist. The methoxy acetyl analogue also exhibited a considerable receptor activation activity in the GTPγS binding assay.

The analogue tetrolicyl-RYYRIK-NH<sub>2</sub> was as active as methylthioacetyl-RYYRIK-NH<sub>2</sub> (Table 2), and angelicyl-RYYRIK-NH<sub>2</sub> was also exhibited considerably high binding activity. However, these analogues containing unsaturated triple and double bonds in the N-terminal acyl group activated the receptor much more (about 10-fold) strongly as compared to isovareloyl-RYYRIK-NH<sub>2</sub>. Apparently, placing the triple and double bonds is disadvantageous to diminish the biological activity, presumably enhancing the hydrophobic interaction to elicit an agonist activity.

L-Val-RYYRIK-NH<sub>2</sub> and D-Val-RYYRIK-NH<sub>2</sub> led considerably reduction of the binding potency to the ORL1-G<sub>αo</sub> receptor. Although these analogues possess the amino group at the C<sub>α</sub> atom of the isovareloyl group, this substitution is apparently disadvantageous to gain a binding potency enough to bind to the receptor. These two peptides also acted as partial agonist. Since L-Val-RYYRIK-NH<sub>2</sub> and D-Val-RYYRIK-NH<sub>2</sub> exhibited almost the same receptor binding potency (Table 2), the configurational difference in arrangement of the alkyl group between L-Val and D-Val did not affect the receptor binding. This means that the isovareloyl group attached to RYYRIK-NH<sub>2</sub> binds to the receptor site with no any stereo-specificity to discriminate the ligand's spatial arrangements.

Table 2. Binding potency of nociceptin, Ac-RYYRIK-NH<sub>2</sub>, isovareloyl- RYYRIK-NH<sub>2</sub> and its analogues for the human ORL1 receptor fused with G<sub>α</sub> protein.

Peptides acyl-RYYRIK-NH <sub>2</sub> (acyl groups)	ORL1 receptor binding potency IC <sub>50</sub> (nM)		
nociceptin	0.60	±	0.08
acetyl	0.79	±	0.18
isovareloyl	7.42	±	0.87
dimethylGlycyl	73.6	±	0.54
methoxyacetyl	2.31	±	0.35
methylthioacetyl	0.74	±	0.21
angelicyl	5.82	±	1.89
tetrolicyl	2.09	±	0.20
L-Val	76.3	±	7.10
D-Val	78.5	±	9.50

In summary, we designed and synthesized seven novel N-terminal acyl-substituted analogues of isovareloyl-RYYRIK-NH<sub>2</sub> to obtain a stronger antagonist and at the same time to clarify the structural elements essential for the receptor binding potency and receptor activation efficacy. The results afforded rather complicated structural information, suggesting the presence very subtle conformational difference between the agonism and antagonism.

### References

1. Meunier, J. C., Mollereau, C., Toll, L., Suaudeau, C., Moisand, C., Alvinerie, P., Butour, J. L., Guillemot, J. C., Ferrara, P., and Monsarrat, B., *et al.* (1995) *Nature*, **377**, 532-535.
2. Dooley, C. T., Spaeth, C. G., Berzetei-Gurske, I. P., Craymer, K., Adapa, I. D., Brandt, S. R., Houghten, R. A., and Toll, L. (1997) *J. Pharmacol. Exp. Ther.*, **283**, 735-741.
3. Burnside, J. L., Rodriguez, L., and Toll, L. (2000) *Peptides*, **21**, 1147-1154.

## The Molecular Mechanism of ORL1 Nociceptin Receptor in Activation: Residual Essentials in the Sixth Transmembrane Domain

Kaname Isozaki<sup>1</sup>, Jinglan Li<sup>1</sup>, Takeru Nose<sup>1</sup>, Tommaso Costa<sup>2</sup>,  
and Yasuyuki Shimohigashi<sup>1</sup>

<sup>1</sup>Laboratory of Structure-Function Biochemistry, Department of Chemistry, Faculty  
and Graduate School of Sciences, Kyushu University, Fukuoka 812-8581, Japan,  
and <sup>2</sup>Laboratorio di Farmacologia, Istituto Superiore di Sanità,  
Viale Regina Elena 299, Roma, Italy  
e-mail: shimoscc@mbox.nc.kyushu-u.ac.jp

*Nociceptin is an endogenous ligand of ORL1 receptor, a member of G protein-coupled receptors. In order to elucidate the molecular mechanism of ORL1 activated by nociceptin, we achieved the complete Ala-substitution series for the transmembrane No. 6 (TM6) in ORL1. This systematic mutagenesis enabled us to identify several amino acid residues crucial for receptor activation, but not for nociceptin binding.*

**Keywords:** site-directed mutagenesis, ORL1 receptor, nociceptin, receptor activation

### Introduction

ORL1 (opioid receptor-like 1) receptor is a seven transmembrane G protein-coupled receptor (GPCR) and couples to G<sub>i/o</sub> protein. Its endogenous ligand is a heptadecapeptide named nociceptin, which produces hyperalgesia and various physiological functions. One of its essential binding sites for nociceptin is an acidic amino acid cluster present in the extracellular loop 2 (EL2) [1]. We discovered the amino acid residues present in the transmembrane domain No. 5 (TM5) as structural elements essential for receptor activation. Those include a cluster of aromatic amino acids on the same ridge of TM5  $\alpha$ -helix [2], and are not involved in the ligand-binding.

Several studies by others have suggested that TM5 is important to hold GPCR in the active conformation by interacting tightly with the adjacent TM6  $\alpha$ -helix [3, 4]. Thus, in this study, we attempted to explore the amino acid residues in TM6 that interact with the TM5 aromatic amino acid(s) essential for driving such an active receptor conformation. We prepared a series of mutant ORL1 receptors, in which 30 amino acids in TM6 (254-285 in rat ORL1 receptor) were all mutated to Ala one by one.

We previously succeeded in the preparation of the ORL1 mutant receptors that were conjugated with G<sub>αo</sub> protein at the C-terminus. These mutants were proved to be excellent in the performance of the GTP $\gamma$ S binding assay. Thus, we also prepared

$G_{\alpha o}$ -fused ORL1 mutant receptors in this study. We here describe that TM6 indeed possesses the amino acid residues important for receptor activation.

## Results and Discussion

In the present study, we combined the two structural strategies important for the structure-function studies of GPCR. The one is Ala-scanning, a screening method that makes it possible to clarify the amino acid residues crucial for receptor activation. The other is  $G_{\alpha o}$ -fusion that affords a GPCR assay system to measure the receptor activation very efficiently. With these two strategies, we attempted to clarify the receptor activation mechanism of ORL1 receptor, especially focusing on the TM6 domain. The site-directed mutagenesis to achieve the Ala-substitution was carried out for all the 30 amino acid residues in TM6 (Fig. 1).

The mutant receptors are hereafter referred to as AxB, where A designates the original amino acid residue at position x of ORL1 and B denotes the amino acid to replace. Each mutant construct was prepared by two-step PCR method, and transiently expressed on the COS-7 cells. Firstly, we quantified the expression levels of receptors by measuring the saturation binding of [ $^3$ H]nociceptin. The Scatchard analysis was carried out for all the mutant receptors to estimate both the dissociation constant ( $K_d$ ) and the receptor protein density ( $B_{max}$ ). The latter shows the amount of receptors that were expressed soundly on the COS-7 cell membranes. As shown in Fig. 2, the P275A mutant receptor exhibited no detectable binding of [ $^3$ H]nociceptin. Although other mutant receptors showed the specific binding, the expression level calculated as  $B_{max}$  was found to be much lower than that of the wild-type ORL1. In particular, those of C272A and L281A were drastically decreased (Fig. 2). The reduction in expression level suggested that the mutated amino acid residue plays an important role in forming a structure proper to the receptor activation. Those

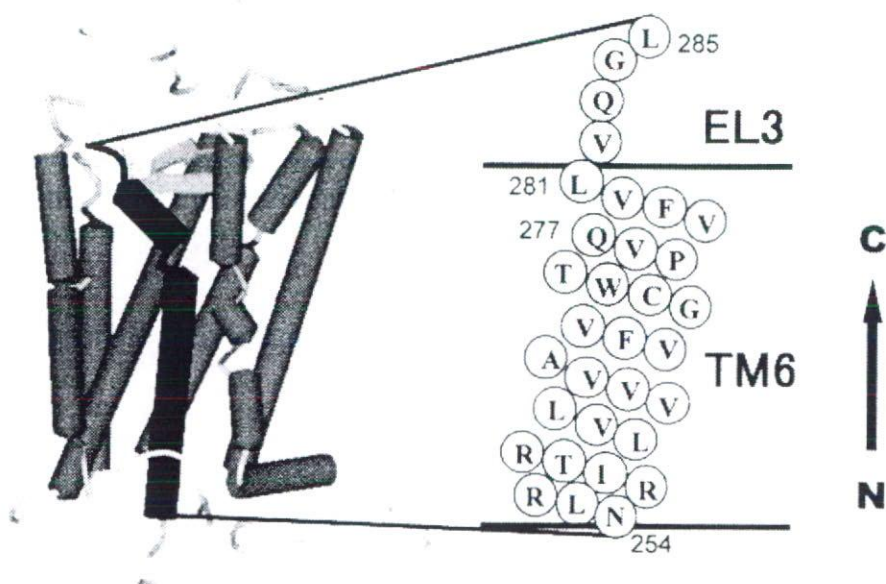


Fig. 1. Putative 3D structure of the rat ORL1 receptor (left) and the amino acid sequences in TM6 and EL3 (right). Amino acids of TM6, 30 in total from Asn254 to Leu285, were all mutated to Ala (except for Ala267). The arrow indicates a direction of the peptide bond main chain.

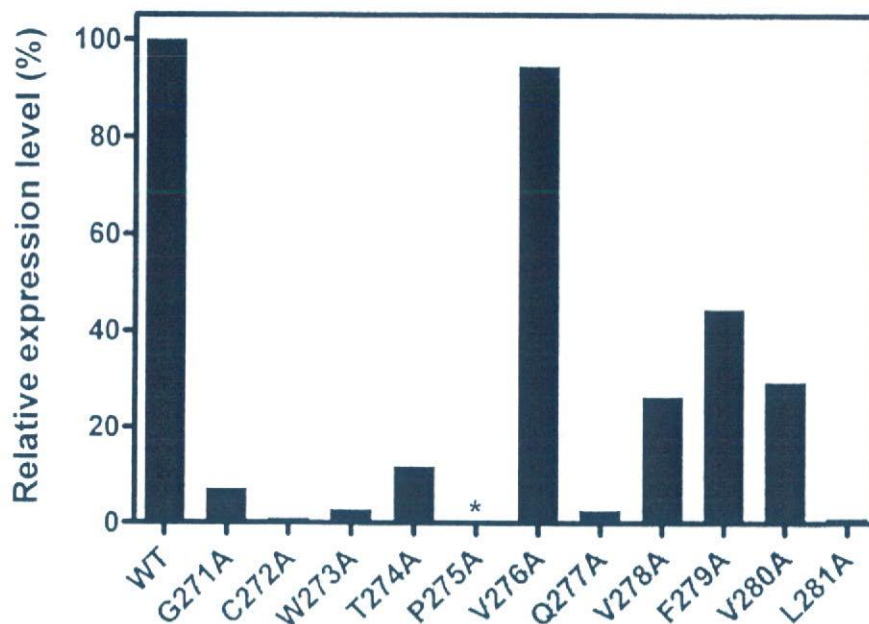


Fig. 2. The relative expression level of the rat ORL1 receptors mutated. Membranes were prepared from COS-7 cells transiently transfected with each mutated receptor- $G_{\alpha o}$  fusion gene. The relative expression levels were calculated by dividing the  $B_{max}$  value of mutant receptors with that of wild-type. \*: Not determined its expression level because of no detectable [ $^3H$ ]nociceptin binding.

membrane preparations were used for the competitive binding assay and GTP $\gamma$ S functional assay, since the dissociation constant  $K_d$  of each mutant receptor was just as good as that of wild-type.

The competitive binding assay was carried out with mutant receptors to assess the binding ability of nociceptin. The binding potency of nociceptin was estimated by calculating the  $IC_{50}$  value. The  $IC_{50}$  values of the mutant receptors were found to be almost comparable to that of the wild-type ORL1. These results suggest that the Ala-substitution does not affect the overall ligand binding sites as observed for TM5 [2]. No assay was performed for P275A mutant receptor because of the lack of specific binding.

To further examine the individual amino acids in nociceptin-selective G protein activation, all mutant receptors were evaluated for their abilities to mediate the nociceptin stimulation of [ $^3S$ ]GTP $\gamma$ S binding. To this end, we used the membrane preparations expressing ORL1- $G_{\alpha o}$  wild-type and mutant receptors. Although all mutant receptors were activated by nociceptin, each mutant receptor produced different maximum response, providing varying  $E_{max}$  and  $EC_{50}$  values. In particular, Q277A showed much lower receptor activation potency and maximal activation level (Fig. 3). This mutagenesis site Q (=Gln) at position 277 is seen only for ORL1 receptor. Other classic opioid receptors possess His instead of Gln at the same position of TM6, and thus it is likely that Gln277 in ORL1 plays a quite unique role in receptor activation. L281A also exhibited much decreased receptor activation (Fig. 3). These results indicate that the extracellular side of TM6 possesses amino acid residues functionally important for the activation (Fig. 1).

One of the purposes of Ala-scanning in this study is to identify the TM6's residue(s) interacting with that (or those) of TM5. In the previous study, we explored several key amino acid residues essential for receptor activation. It should be noted

that those residues (F212, F217, and F221) locate at the similar edge of TM5  $\alpha$ -helix [2]. Thus, we decided to exemplify such a putative interaction between the TM  $\alpha$ -helices by focusing on the TM6 adjacent to TM5.

Using the crystal structure of bovine rhodopsin (PDB ID code: 1F88) as a template, we constructed initial 3D structure of the ORL1 receptor by the homology modeling procedure. In the modeling structure, two TM6 residues were assumed to interact with the key residues of TM5 at the extracellular side. One is Gln277 and the other is Leu281. These two residues are highly likely to interact with Phe221 and Phe217 in TM5, respectively, since the distance between two functional side-chains was calculated to be within 3.5 Å. When Gln277 was replaced to Ala, the binding potency to nociceptin was almost unchanged, but it decreased all the parameters related to receptor activation, such as the basal activity, activation efficacy, and maximal activation level. Similar results were also observed in the L281A mutation. From these results, we can hypothesize that Gln277 and Leu281 are interacting with Phe221 and Phe217 presumably by the NH/ $\pi$  and CH/ $\pi$  interaction, respectively. These interactions must be with relation, for example, to the change in receptor conformation from the inactive state to the active state.

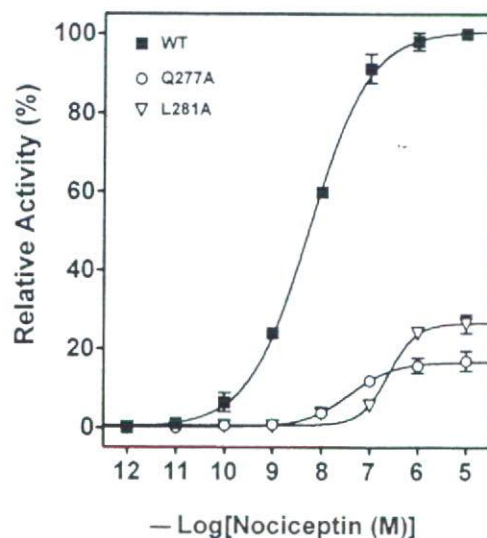


Fig. 3. Dose-response curves of nociceptin in the [ $^{35}$ S]GTP $\gamma$ S binding assay using the mutant receptors. The two typical mutated receptors of Q277A and L281A are shown. Responses are given as percentage changes from the wild-type (WT).

## References

1. Okada, K., Kawano, M., Isozaki, K., Chuman, Y., Fujita, T., Nose, T., Costa, T., and Shimohigashi, Y. (2003) *Peptide Science 2002*, 261-264.
2. Isozaki, K., Okada, K., Koikawa, S., Nose, T., Costa, T., Shimohigashi, Y. (2006) *Peptide Science 2006*, 11.
3. Mollereau, C., Moisand, C., Butour, J. L., Parmentier, M., and Meunier, J. C. (1996) *FEBS Lett*, **395**, 17-21.
4. Pignatari, G. C., Rozenfeld, R., Ferro, E. S., Oliveira, L., Paiva, A. C. M., and Devi, L. A. (2006) *Bio. Chem*, **387**, 269-276.

# A Docking Modelling Rationally Predicts Strong Binding of Bisphenol A to Estrogen-Related Receptor $\gamma$

Takeru Nose\* and Yasuyuki Shimohigashi

Laboratory of Structure-Function Biochemistry, Department of Chemistry, Faculty of Sciences, Kyushu University, Fukuoka 812-8581, Japan

**Abstract:** A computer-aided docking study was carried out to quickly clarify the binding structure of the ligand-receptor complex between bisphenol A (BPA), a well-known endocrine disruptor, and estrogen-related receptor  $\gamma$  (ERR $\gamma$ ). The resulting complex indicated that BPA binds to the ligand-binding pocket of ERR $\gamma$  without any disruptions of the activation conformation.

**Keywords:** Estrogen-related receptor  $\gamma$ , bisphenol A, endocrine disruptors, docking calculation.

## INTRODUCTION

Endocrine disrupting chemicals (EDCs) are chemicals that mimic the effects of hormones and thereby disrupt endocrine systems. Numerous common industrial chemicals are suspected of being EDCs. Bisphenol A (BPA), 2,2-bis(4-hydroxyphenyl)propane, is a strong EDC candidate. BPA is now important as a raw material for epoxy resins and polycarbonate plastics. In 1993, Krishnan *et al.* reported that BPA leaked from a flask made of polycarbonates and caused abnormal growth of MCF-7 human breast cancer cells by mimicking the activity of the native estrogen 17 $\beta$ -estradiol (E2) [1]. Also, Gaido *et al.* described that BPA as well as E2 exhibited transactivation activity in a yeast-based estrogen receptor gene transcription assay [2]. Although the activities of these BPAs were much weaker than that of E2 (1/5,000 to 1/15,000 of the activity of E2), BPA was acknowledged as one of the EDCs that act upon estrogen receptor (ER).

Nuclear receptors are a family of 48 or more intracellular receptors in humans. Estrogen-related receptor (ERR) is a subfamily of human nuclear receptors closely related to ER [3–5]. In spite of their high homology to ER, ERR members do not respond to E2, and constitutively activate the transcription in eukaryotic cells. Meanwhile, vom Saal *et al.* have extensively documented numerous low-dose effects of BPA [6]. The low-dose effects of BPA have also been reported by many other groups (for review vom Saal *et al.* [7]); for example, Belcher *et al.* reported that BPA disrupts neural development in the rat fetus [8]. For these low-dose effects of BPA, it has been thought that ER is a target receptor. However, Takayanagi *et al.* reported recently that BPA strongly binds to ERR $\gamma$  [9]. These results raise the possibility that BPA may be an EDC of ERR $\gamma$  possessing unidentified activity. Thus, this unpredictable strong binding potency of BPA has underscored the need for development of a new rapid procedure to assess the risk posed to all nuclear receptors.

As a strategy to screen a large number of chemicals with or without endocrine disruption potentials, studies on the quantitative structure-activity relationship (QSAR) have been carried out, especially for ER [10–12]. Recently, computational docking operation becomes a useful vehicle for investigating the molecular binding interactions [13–27]. Advances in three-dimensional (3D) modeling and docking strategies allow the application of *in silico* structure-based drug design studies (SBDD) to such assessments. These were originally designed to predict how small molecules such as ligands or drug candidates bind to a receptor whose 3D structure has been clarified. Indeed, if an *in silico* EDC screening system based on SBDD was available, such a system could perform a high-speed screening of chemicals against nuclear receptor-LBDs, thereby providing an effective risk assessment without the need for costly and time-consuming wet experiments.

The present study aims to examine the question of how BPA docks with the LBD, based on the fact that BPA shows strong binding activity to ERR $\gamma$ . Heretofore, the attention has been paid to the sex steroid hormone receptors ER and AR as targets of EDCs. However, the binding of BPA to ERR $\gamma$  invokes to involve all the nuclear receptors to investigate. In this report, we performed computer-aided docking studies on the BPA and ERR $\gamma$ -LBD complexes to clarify the structural essentials by which they bind to each other. The complex structure of BPA/ERR $\gamma$ -LBD, which was calculated in this study, successfully described its high constitutive activity. BPA bound to ERR $\gamma$  has been found as a quite unique space-filler in the ligand-binding domain.

## MATERIALS AND METHOD

3D structures of BPA and other ligands were constructed by the program Sketch, one of the modules of Insight II (Accelrys, San Diego, CA). In order to prepare the receptor molecule appropriately in the docking calculation, hydrogens were added onto heavy atoms identified by X-ray crystallography (1TFC), and the charges were assigned by Biopolymer module in the neutral condition. CFF91 force field (Accelrys) was used in all molecular mechanics calculations. For

\*Address correspondence to this author at the Laboratory of Structure-Function Biochemistry, Department of Chemistry, Faculty of Sciences, Kyushu University, 6-10-1 Hakozaeki, Higashi-ku, Fukuoka 812-8581, Japan; Tel: +81-92-642-2585; Fax: +81-92-642-2585; E-mail: nosescc@mbox.nc.kyushu-u.ac.jp

calculation of the volume of the ligand-pocket, the 3D structure of apo-form ERR $\gamma$ -LBD (1TFC: PDB code) was used [28]. The volume size of vacant ligand-pocket was estimated and determined by means of an active site finding tool called Binding Site Analysis (Accelrys). Using volume keyword, molecular volumes were computed by Gaussian 03 equipped with 6-31G basis set, following energy minimization step [29]. Structural formulas of all the ligands used in this study are shown in Fig. 1.

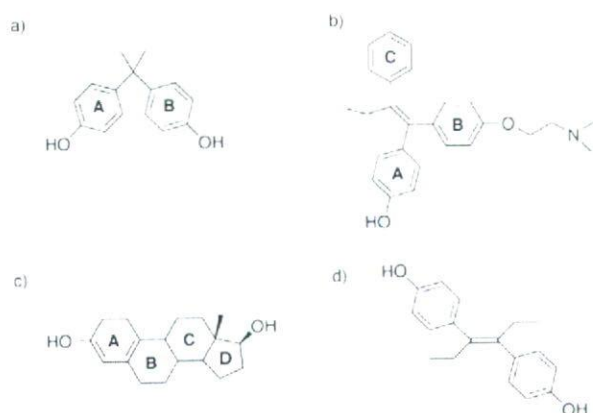


**Figure 1.** The structural formulas of bisphenol A (BPA), 4-hydroxytamoxifen (4-OHT), 17 $\beta$ -estradiol (E2), and diethylstilbestrol (DES). a: BPA, BPA possesses the two phenol groups A and B together with the two methyl groups. b: 4-OHT, 4-OHT possesses three benzene rings on the trans-ethylene double bond: i.e., A, phenol; B, *p*- $\beta$ -dimethylethoxyphenyl; and C, phenyl rings. c: E2, and d: DES.

Docking calculations between BPA and ERR $\gamma$ -LBD (1TFC) were carried out by using Affinity program (Accelrys) in grid docking methodology with CFF91 force field on SGI O2 workstation [30, 31]. The flexible region of the docking calculation includes the BPA molecule initially placed and all the residues in an 8 Å-surrounding distance in the ligand pocket of LBD. BPA was placed at three different positions by referring to the structure of 4-OHT in the 4-OHT/ERR $\gamma$ -LBD complex (1S9Q) [28].

With the aim of binding energy calculation of BPA in each complex, 6-31G level *ab initio* FMO-MP2 calculations were performed by ABINIT-MP (Advanced Soft, Tokyo, Japan) with BPA and amino acid residues of ERR $\gamma$ -LBD being within 6 Å from BPA [32-35]. FMO calculations were carried out on a parallel UNIX server, IBM eServer p5 model 595, at the computing and communications center of Kyushu university. The binding energies ( $\Delta E$ ) between BPA and ERR $\gamma$ -LBD were calculated from the computed results of the FMO calculations by the method described by Fukuzawa *et al.* [36]. Binding energy ( $\Delta E$ ) between BPA and ERR $\gamma$ -LBD can be expressed in the equation 1 as the difference in each energy value of the receptor ( $E_{\text{receptor}}$ ), ligand ( $E_{\text{ligand}}$ ), and complex ( $E_{\text{complex}}$ ) [36].

$$\Delta E = E_{\text{complex}} - (E_{\text{receptor}} + E_{\text{ligand}}) \quad (1)$$

## RESULTS AND DISCUSSION

ERR $\gamma$  is a constitutively active and orphan receptor. Although no natural ligand is known, ERR $\gamma$  is deactivated by DES and 4-OHT [37-29]. To date, the data on five 3D structures of ERR $\gamma$ -LBD have been deposited in the RCSB-protein data bank. Two of the five structures explain the non-liganded apo-form [28, 40], and the other three structures show the holo-structures of ERR $\gamma$ -LBD bound with either 4-OHT or DES [28]. In order to discuss the probability of BPA binding with ERR $\gamma$ -LBD, we first calculated the volume of the ligand-pocket of ERR $\gamma$ -LBD and the molecular volume of BPA. Since the binding sites of 4-OHT and DES in ERR $\gamma$ -LBD have been determined to be the same by the X-ray crystal analysis, we first selected the one as a putative ligand binding pocket for BPA. The volume size of vacant ligand space in the apo-form ERR $\gamma$ -LBD was calculated to be 293.6 Å<sup>3</sup>. The molecular volume of BPA was computed precisely by using the volume keyword in Gaussian 03 and the calculated volume was 295.2 Å<sup>3</sup>. Although the program Binding Site Analysis provided several other pockets, their volume sizes were much smaller than BPA's molecular size.

As a result, we could obtain compatible values for volumes of the ligand and the receptor. Based on this finding, BPA was judged to have a sufficient volume to bind to the vacant space of the ERR $\gamma$ -LBD apo-form.

To examine how BPA binds to ERR $\gamma$ -LBD, flexible docking calculations were carried out using the program Affinity (Accelrys) with the apo-form ERR $\gamma$ -LBD (1TFC) as a template [30, 31]. In this study, BPA was manually placed at three different positions by referring to the structure of 4-OHT in the 4-OHT/ERR $\gamma$ -LBD complex (1S9Q) before the docking calculation [28]. As shown in Fig. 1 and 2, 4-OHT possesses 3 different aromatic rings, namely, the phenol (A-ring), the *p*- $\beta$ -dimethylethoxyphenyl (B-ring) and the phenyl (C-ring) on the trans-ethylene double bond. BPA has two phenol groups (A and B) on the sp<sup>3</sup>-carbon atom. Placing the A-ring of BPA at the point where the A-ring of 4-OHT is located, we attempted to place the B-ring of BPA at the points corresponding to the point where the B- or C-ring of 4-OHT is located. In addition to these two arrangements, we further attempted to place BPA to take the initial positioning with the B- and C-rings of 4-OHT. From each docking calculation, 5-7 different structures of the BPA/ERR $\gamma$ -LBD complex were obtained, and their affinity scores are listed in Table 1.

Complexes 1-7, 2-3, and 3-6 gave the best affinity score in each calculation, and we selected these as the representative complexes. When BPA was placed at random in the LBD, the Affinity docking calculations resulted in the structures similar to 1-7 and 2-3. Since these structures never gave the Affinity scores greater than 1-7 and 2-3, we just selected the complexes 1-7, 2-3, and 3-6 as the structures for further examinations.

Fig. 3 illustrates these selected docked structures of BPA. It should be noted that BPA has almost the same position in each of these docked structures, even though the calculations were initiated from completely different placements of BPA. The binding structure of 2-3 is almost completely compatible to that of 3-6, although BPA in 1-7 is in a different orientation. In particular, one of the methyl groups of 1-7, the left

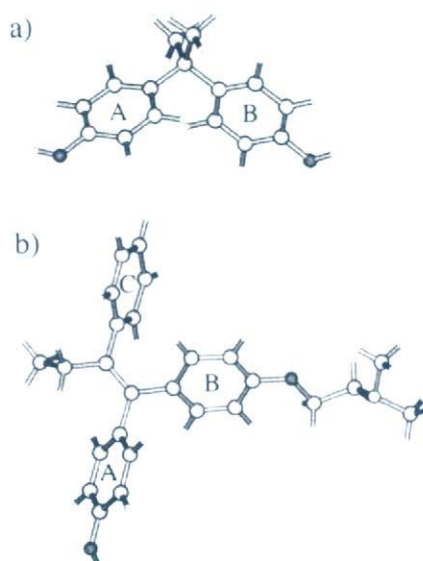


**Figure 2.** The three dimensional structures of bisphenol A (BPA) and 4-hydroxytamoxifen (4-OHT). a: BPA is shown by its minimum energy conformation. b: 4-OHT is shown by the structure pulled out from the 4-OHT/ERR  $\gamma$ -LBD complex (1S9Q). Characters (A and B in 'a') and A, B and C in 'b') indicated the same ring structures as shown in Fig. 1.

side methyl group ( $\alpha$  in Fig. 3a), was found to be apart from that of 2-3 (Fig. 3). As a result, the methyl group  $\alpha$  of 1-7 is located in the hydrophobic pocket constructed by Met306, Leu309, and Ile310. On the other hand, the methyl group  $\alpha'$  of 2-3 (Fig. 3b) is in close proximity to the benzene ring of Phe450 ( $< 3.1 \text{ \AA}$ ), which may be responsible for the CH/ $\pi$  interaction. These results clearly indicate that the pocket or vacant space available for BPA is uniform and there are only a limited number of attachment positions by which BPA can occupy it.

We preliminary carried out the Affinity docking calculations to complex BPA into other templates derived from ERR $\gamma$ -LBD/4-OHT or DES (1S9Q or 1S9P). However, the resulting BPA-binding structures were found to leave a considerably large empty space, with the activation function (AF)-containing H12 being in deactivation conformation. Apparently, this is inappropriate to explain BPA's high binding affinity and high basal constitutive activity.

For detailed comparison of the binding energies of BPA in these three BPA/ERR $\gamma$ -LBD complexes, we carried out *ab initio* (HF and MP2 level) calculations by the fragment molecular orbital (FMO) method [32-36]. As shown in Table 2, HF and MP2 calculations afforded the results of negative  $\Delta E$  values for BPAs, indicating a structural stabilization due to the ligand binding. Such negative  $\Delta E$  values reveal that BPA is a favorable binder of ERR $\gamma$ , as 4-OHT and DES are.

**Table 1.** Results of the Flexible Docking Calculations of Bisphenol A (BPA) to the ERR $\gamma$ -LBD apo-form by the Computer Program Affinity

Complex No. <sup>a</sup>	Number of Appearances <sup>b</sup>	Energy (kcal/mol)	Ranking
1-1	9	-864.683	7
1-2	16	-887.407	6
1-3	15	-887.565	5
1-4	13	-890.651	3
1-5	33	-890.461	4
1-6	15	-898.950	2
1-7	13	-898.996	1
2-1	7	-921.715	5
2-2	20	-928.930	4
2-3	18	-930.596	1
2-4	14	-930.595	2
2-5	30	-928.931	3
3-1	6	-842.793	5
3-2	4	-848.302	4
3-3	1	-840.223	6
3-4	1	-880.767	3
3-5	26	-882.895	2
3-6	33	-882.896	1

<sup>a</sup>Complex number 1, 2, and 3 represent the calculations started from different initial positionings, respectively. In complex 1, the phenol rings of BPA are placed at the positions of the A- and B-rings of 4-OHT (see Fig. 2). Complex 2 is placed in the positions of the A- and C-rings, and complex 3 is placed in the positions of the B- and C-rings.  
<sup>b</sup>It means the times appeared as the result in each affinity calculation.

To compare the binding energy of BPA with that of a weak binder, we selected E2, an endogenous ligand of ER. Flexible docking calculations between E2 and ERR $\gamma$ -LBD (1TFC) followed by FMO calculations were carried out. It was found that E2 exhibits  $\Delta E$  value of +19.8 kcal/mol, which is much larger than those of binders 4-OHT, DES and BPA in the HF calculation (Table 2). This is a demonstration that E2 is indeed a weak binder of ERR $\gamma$ . This notably large

$\Delta E$  value obtained by the HF calculation indicates that there was an unfavorable spatial contact and conformation change along with a complex formation between E2 and ERR $\gamma$ -LBD. In the calculated E2/ERR $\gamma$ -LBD complex, the steroid structure of E2 in a planer configuration warped almost 45 degree at the B-ring. The ligand binding pocket of ERR $\gamma$ -LBD (1TFC) was too small to bind E2.

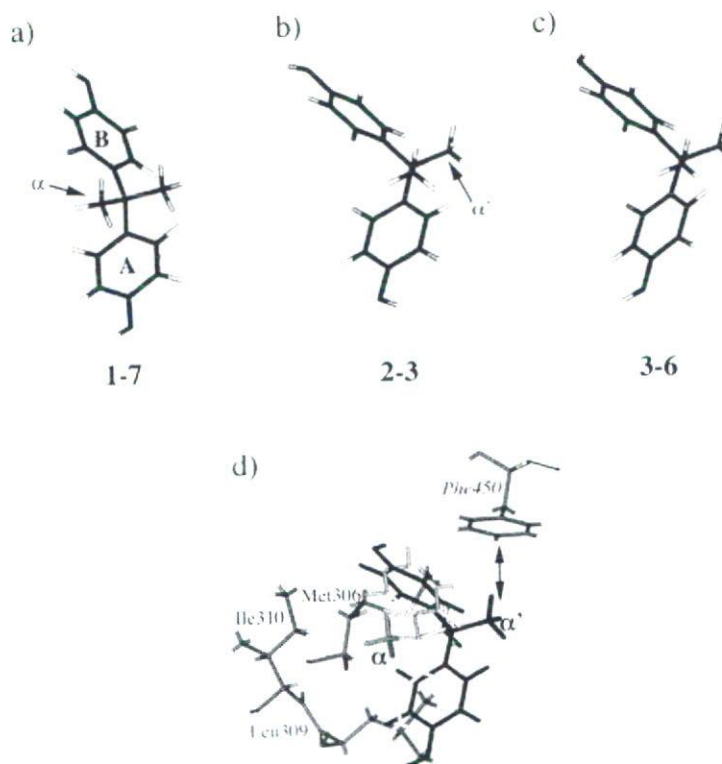


**Figure 3.** The three-dimensional structures of bisphenol A (BPA) docked in the apo-form ERR $\gamma$ -LBD. Each structure (a)-(c) was obtained by calculations starting from different dockings with initial placements. The calculations were carried out by the computer program Affinity. 1-7 (a), 2-3 (b), and 3-6 (c) show the structure of BPA (bold sticks) obtained with the best Affinity score (see Table 1). In each calculation, the other structures of BPA are shown by thin stick lines. A and B are labeled on the two phenol rings of BPA.  $\alpha$ : The methyl group on the left side of 1-7; and  $\alpha'$ : Another methyl group on the right side of 2-3. (d) Structural comparison of 1-7 (white molecule) and 2-3 (black molecule). All amino acid residues were from the results of 1-7, with the only exception being *Phe450* from the results of 2-3.  $\alpha$  and  $\alpha'$  are described above.

**Table 2.** Calculated Binding Energies ( $\Delta E$ ) of the ERR $\gamma$  Complexes with BPA, 4-OHT, DES and E2 by *ab initio* Calculations

Complex (No.)	$\Delta E$ (HF)	$\Delta E$ (MP2)
1TFC+BPA (1-7)	-7.90	-57.6
1TFC+BPA (2-3)	-14.4	-68.8
1TFC+BPA (3-6)	-0.14	-48.1
1S9Q (4-OHT) <sup>a,b</sup>	-10.6	-82.4
1S9P (DES) <sup>a</sup>	-4.03	-64.5
1TFC+E2	19.8	-49.3

Energies are in kcal/mol.

<sup>a</sup>Crystal Structure, in which water molecule(s) are ignored. <sup>b</sup>A cholic acid, closely existed with 4-OHT in 1S9Q, regarded as a part of the receptor molecule in the calculations.